



Orientation invariant ECG-based stethoscope tracking for heart auscultation training on augmented standardized patients

Nahom Kidane¹, Salim Chemlal², Jiang Li², Frederic D. McKenzie¹ and Tom Hubbard³

Abstract

Auscultation, the act of listening to the heart and lung sounds, can reveal substantial information about patients' health and other cardiac-related problems; therefore, competent training can be a key for accurate and reliable diagnosis. Standardized patients (SPs), who are healthy individuals trained to portray real patients, have been extensively used for such training and other medical teaching techniques; however, the range of symptoms and conditions they can simulate remains limited since they are only patient actors. In this work, we describe a novel tracking method for placing virtual symptoms in correct auscultation areas based on recorded ECG signals with various stethoscope diaphragm orientations; this augmented reality simulation would extend the capabilities of SPs and allow medical trainees to hear abnormal heart and lung sounds in a normal SP. ECG signals recorded from two different SPs over a wide range of stethoscope diaphragm orientations were processed and analyzed to accurately distinguish four different heart auscultation areas, aortic, mitral, pulmonic and tricuspid, for any stethoscope's orientation. After processing the signals and extracting relevant features, different classifiers were applied for assessment of the proposed method; 95.1% and 87.1% accuracy were obtained for SP1 and SP2, respectively. The proposed system provides an efficient, non-invasive, and cost efficient method for training medical practitioners on heart auscultation.

Keywords

ECG analysis, auscultation, standardized patients, virtual pathology, medical training

1. Introduction

Cardiac examination (CE) can accurately detect most structural cardiac abnormalities in a differential diagnosis if performed properly. Ensuring proper examination requires competent training in cardiac inspection, palpation, and auscultation. However, nowadays most hospital admissions are short and intensely focused with fewer opportunities for trainees to learn and practice bedside examination skills.¹ Hence, sophisticated manikins have been widely used as patient simulators mimicking a number of cardiovascular indices and improving CE training, but cannot replace contact with actual patients.¹ Over the past few decades, standardized patients (SPs), who are healthy individuals trained to portray real patients with specific illnesses and conditions, have been widely used in clinical training.² SP-based encounters have shown to improve patient assessment, counseling, and clinical skills of medical trainees.^{2–5} However, the range of symptoms and syndromes they can physically portray stays limited

since they are typically healthy patient actors. Augmenting SPs with the ability to simulate a large number of abnormalities would enhance the experience and variety of symptoms medical students can encounter.⁶ For cardiac auscultation (CA) for instance, this is achieved by modifying the stethoscope.

Electrocardiography (ECG) detects and records physiological signals generated by electrical changes that occur in the body. Most ECG related research focus on automated signal processing for physiological states

¹Department of Modeling, Simulation, and Visualization, Old Dominion University, Norfolk, VA, USA

²Department of Electrical and Computer Engineering, Old Dominion University, Norfolk, VA, USA

³Eastern Virginia Medical School, Norfolk, VA, USA

Corresponding author:

Rick McKenzie, ECSB 1303 Department of Modeling, Simulation and Visualization Engineering, Norfolk, VA 23529, USA.

Email: rdmckenz@odu.edu

monitoring and diagnosis of heart abnormalities;^{7–10} however, using ECG for virtual pathology stethoscope (VPS) tracking has not been much investigated. VPSs are devices that substitute normal heart or lung sounds with abnormal auscultatory findings from actual patients with a variety of diseases. McKenzie et al.¹¹ designed a VPS that can automatically play abnormal sounds by tracking the location of the stethoscope over the SP's torso. The prototype utilized a tiny magnetic sensor attached on the chest piece of the VPS for tracking purposes; however, the system was complex, noisy, and very costly.

The goal of our research is to improve CA skills of medical students with virtual pathology simulation using modified stethoscopes in tandem with SPs. A cost-efficient and orientation-invariant tracking method for simulating virtual symptoms in desired auscultation areas would extend SPs capabilities allowing medical student trainees to perform a more realistic CA.

In this work, we aim to detect the stethoscope location at four auscultation areas: aortic, pulmonic, mitral and tricuspid. We have previously shown that ECG can distinguish these areas when limiting the orientation of the stethoscope to only one angle.⁶ Here, we prove that ECG can further be used for identifying the four areas even with a wide range of stethoscope orientations, which is more practical since trainees would evidently hold the stethoscope differently during auscultation. The method involves preprocessing ECG signals, extracting a multitude of attributes, and identifying a subset of relevant features. Five different classifiers, naive Bayes, Bayes network, *k*-nearest neighbor, multilayer perceptron, and C4.5 decision tree, are utilized for VPS tracking assessment of the discriminative abilities and orientation invariability of the system. The proposed tracking method is considered to be non-invasive, natural and cost-effective.

The remainder of this paper is organized as follows. Section 2 provides background information on auscultation areas and ECG mechanics. Next, Section 3 reviews the state of the art in auscultation training simulation, and compares various simulators underlining the benefits of hybrid simulation, such as our proposed VPS system. Section 4 describes the proposed methodology and implementation steps; it includes data collection, preprocessing, feature extraction, feature selection, and classification. Section 5 reports on the results. Finally, Section 6 concludes with a summary discussion and possible directions for future work.

2. Background

2.1. Auscultation areas

CA, or listening to the heart's sound, provides vital clues for diagnosing most cardiac anomalies. Cardiac diseases and conditions, such as congestive heart failure, systemic

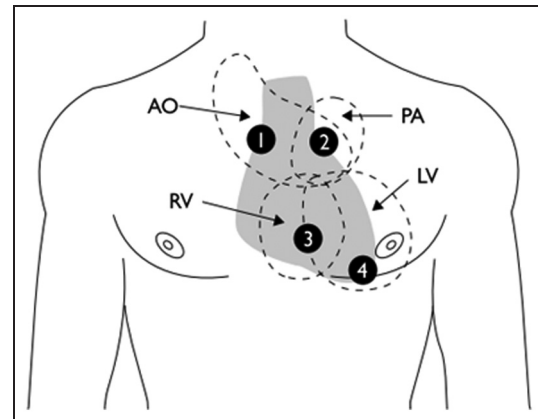


Figure 1. Points of auscultation. AO = aortic area; LV = left ventricle; PA = pulmonic area; RV = right ventricle; 1 = right second intercostal space; 2 = left second intercostal space; 3 = midleft sternal border (tricuspid); 4 = fifth intercostal space, midclavicular line (mitral).¹²

arterial hypertension, coronary artery disease, and valvular heart disease can be detected through abnormal auscultatory findings.¹² Although most of these diseases are now identified using advanced technologies, such as echocardiography, auscultation remains the safest, most convenient, and least expensive diagnosis method.¹²

Points of auscultation over the precordium, which is the portion of the body over the heart and lower chest, are generally correlated with cardiac valves (Figure 1).¹² Placement of the stethoscope's diaphragm on these areas may reveal heart murmurs associated with valvular abnormalities.

2.2. ECG mechanics

The electrical activities of the cells generate current flow within the body and results in a potential difference on the surface of the skin.¹³ These potential differences can be measured by surface electrodes attached to the outer body surface. An electrocardiograph amplifies and records these signals as they travel throughout the body.

Normal ECG recoding produces distinct waveforms that represent the cardiac cycle phases, as shown in Figure 2. The deflections in ECG signal are marked alphabetically by P, Q, R, S, and T. The P wave represents the atrial depolarization; QRS complex represents ventricular depolarization; and T wave represents ventricular repolarization. U wave may follow the end of the T wave, but it is either absent or difficult to identify on typical ECG readings.^{7,13} The vertical displacement, referred to as amplitude, represents the magnitude of the electrical signal propagated by the myocardium, while the horizontal displacement, referred to as duration, represents the time duration of the electrical activity.

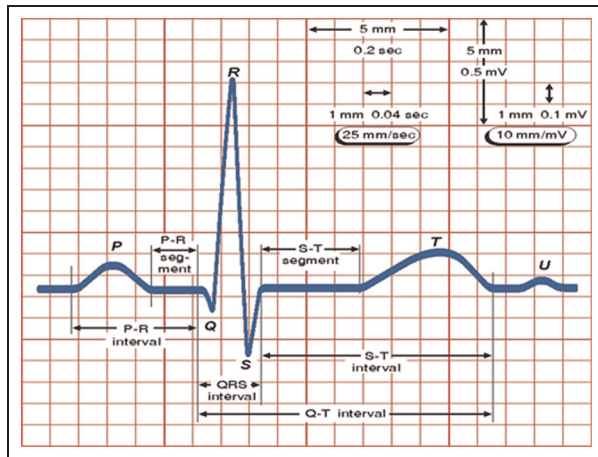


Figure 2. Typical fiducial points and possible features for a normal ECG signal.¹³

3. State of the art

The teaching of CA has been an area of recognized importance since the inception of the stethoscope.^{14,15} Various simulation technologies, with varying degrees of sophistication, have been developed and adapted in CA training and evaluation. For instance, diverse computer based simulators ranging from simple CD-ROM recordings to highly interactive web-based virtual patients (VPs) are regularly utilized for CA teaching. Several studies^{16–18} investigating the performance of such simulators have shown significant improvement on medical students' CA abilities; however, auscultation requires processing multiple senses simultaneously, such as listening and palpating for correct auscultation areas, which cannot be effectively taught with passive hearing or limited software interaction.

Computer-enhanced manikins consisting of full or partial replications of the human anatomy offer enhanced modalities for teaching both active and passive CA skills. Most mid- to high-fidelity manikins allow the learner to hear pre-recorded heart/lung sounds by placing a stethoscope at the external landmark over their plastic torsos.¹⁹ The cardiology patient simulator (CPS) or 'Harvey' is the earliest of this type; it is a high-fidelity, partial-body trainer fixed in the supine position.^{19,20} Harvey can simulate 30 pre-recorded heart and lung sounds through a speaker mounted inside the plastic chest wall.^{21,22} The educational efficacy of Harvey has been rigorously tested by many researchers²¹ and has shown significant improvement on CA training. Many other similar upright partial body manikins are commercially available, such as Lung Sound Auscultation Trainer (LSAT), Student Auscultation Manikin (SAM), and Life/form[®] auscultation trainer and Smartscope[™] system.^{21,22} CA can also be taught with high-fidelity full-body manikins, such as Laerdal's Medical SimMan 3G, which contains sophisticated

mechanics for simulating palpable pulse, spontaneous breathing and altered speech.¹⁹

All of these various types of simulators may enable clinicians at any level to learn, practice and master their CA skills, although they each have their own limitations. As mentioned by Ward and Wattier,¹⁹ most speaker-based manikins lack in the range and accuracy of anatomical sounds they produce; the sounds played are 'read-only' and cannot be replaced in real-time by other sounds. Furthermore, speakers are limited in number and require exact stethoscope placement to work properly. Environmental noises can also lead to distractions and hinder the realism of the simulation scenarios. In addition to the built-in limitations, these simulators are inanimate objects.

A hybrid simulation using SPs and virtual pathology simulators would drastically add realism to auscultation training. The feasibility of such integrated simulations has been studied in other clinical settings^{23,24} and has shown considerable improvement in trainees' patient interaction and assessment skills. McKenzie et al.¹¹ applied a hybrid simulation to augment abnormal auscultatory findings in real-time using VPS across common auscultation areas on a healthy SP. However, their magnetic-based VPS tracking system was complex, expensive and susceptible to electrical and metallic interference. Such system consisting of live and virtual training allows a more realistic CA simulation.

In the past two decades, several studies have assessed the potential of ECG in human biometrics^{25–27} and emotion modeling.^{8,9} Nevertheless, the potential of ECG signals for VPS tracking has not been elsewhere investigated. In our previous study,⁶ we carried out initial preliminary work on the feasibility of such an ECG based approach for VPS tracking. The previous proposed method involved analyzing ECG signals recorded at the four aforementioned auscultation areas of a single SP with the stethoscope diaphragm positioned at the same orientation. The proposed method was accurately able to distinguish between the different areas; however, having the diaphragm at the same orientation is not practical for medical training as different individuals would obviously hold and place a stethoscope differently. In this work, we propose a stethoscope orientation-invariant method for identifying the four heart auscultation areas on the human body based on ECG signal analysis.

4. Methods

The composition of the proposed system procedure is shown in Figure 3. The respective descriptions are provided in this section.

4.1. Data collection

Two direct-contact electrodes fixed on an acoustic stethoscope recorded ECG signals from the auscultation

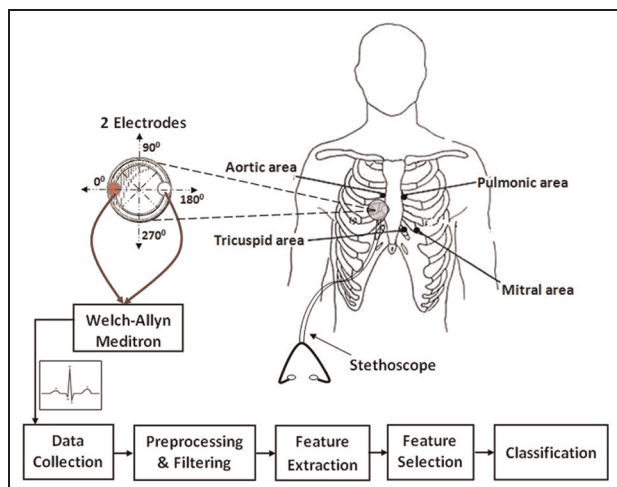


Figure 3. System overview.

landmarks of a SP's chest. Although using multi-lead systems may increase signal- to-noise ratio, noise rejection, and redundancy for accurate diagnostic evaluation,⁷ they are inconvenient and uncomfortable for non-clinical applications, as is the case for our research. Our intent is to provide high realism to increase the likelihood of trainees to suspend disbelief; therefore, the least number of leads allows us to better hide the encroaching technology. Our setup comprises a single-lead ECG configuration, which have shown promising results on biometric applications and delivers relative accuracy for non-diagnostic monitoring applications.^{25,27}

Two male SPs aged 25 and 27, from Eastern Virginia Medical School's Sentara Center for Simulation and Immersive Learning, were recruited for data collection.

Using WelchAllyn Meditron analyzer, ECG signals were acquired at 44.1 kHz with 16 bits per sample. For angular variations, signals were collected by rotating the stethoscope diaphragm clockwise with increments of 45°, producing 8 different orientations for each auscultation area. In addition, 5 runs were collected for each angle; thus, resulting in a total of 40 ECG signals for each auscultation area. Each run composed of about 10 pulses; however, first and last pulses were always removed since they tend not to contain entire segments and waves. For instance, the recording may start within a P wave as it may also end within a T wave. This condition will later ensure extracting equal number of features for all pulses. All recordings were performed in a quiet room with the subjects maintaining a relaxed seated upright position.

4.2. ECG preprocessing

ECG frequency ranges from DC to 1 kHz;⁷ therefore, our initial preprocessing step was to reduce the over-sampled

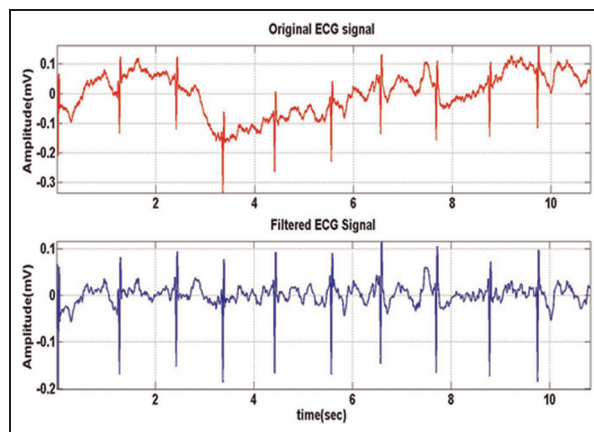


Figure 4. A sample ECG run of pulmonic region of SPI before and after filtering, top and bottom plots, respectively.

temporal data. Considering Nyquist sampling criterion, which mandates sampling at a rate of at least twice the highest desired frequency to avoid aliasing, the recorded ECG signals were down-sampled from 44.1 kHz to 2 kHz.

ECG signals are often contaminated by various kinds of noises and artifacts, which may have similar morphological behavior and frequency range as the characteristic waveforms.⁷ The main noise categories are low-frequency baseline wandering caused by respiration and body movements, and high-frequency random noises (50–60 Hz) caused by power line interference and muscle contraction.²⁸ These artifacts severely limit the utility of recorded ECG signals; therefore, denoising is vital for ECG analysis.

To remove the high-frequency power line noise, an eighth-order zero-phase (bidirectional) Butterworth low-pass filter with 40 Hz cut-off frequency was utilized.²⁸ On the other hand, for baseline wandering noises and low-frequency artifacts, we applied a high-pass first-order FIR filter with a cut-off frequency of 0.7 Hz.²⁸ Figure 4 shows an original ECG run (top plot) recorded at the pulmonic area of SPI and the resulting signal after filtering (bottom plot).

4.3. Feature extraction

Feature extraction provides fundamental attributes (amplitudes and intervals) to be used in subsequent ECG analysis. The QRS complex is a well-recognized wave from within the ECG and serves as the starting point for automated diagnosis and classification schemes.²⁹ There are several diverse and sophisticated algorithms for QRS detection; Kohler et al.²⁸ investigated the performance of various QRS detection methods and classified them based on their detection accuracy and computational cost. Based on these latter results, Pan–Tompkins algorithm²⁹ was selected for our detection; it is a relatively low computational yet highly accurate QRS-detection method. The

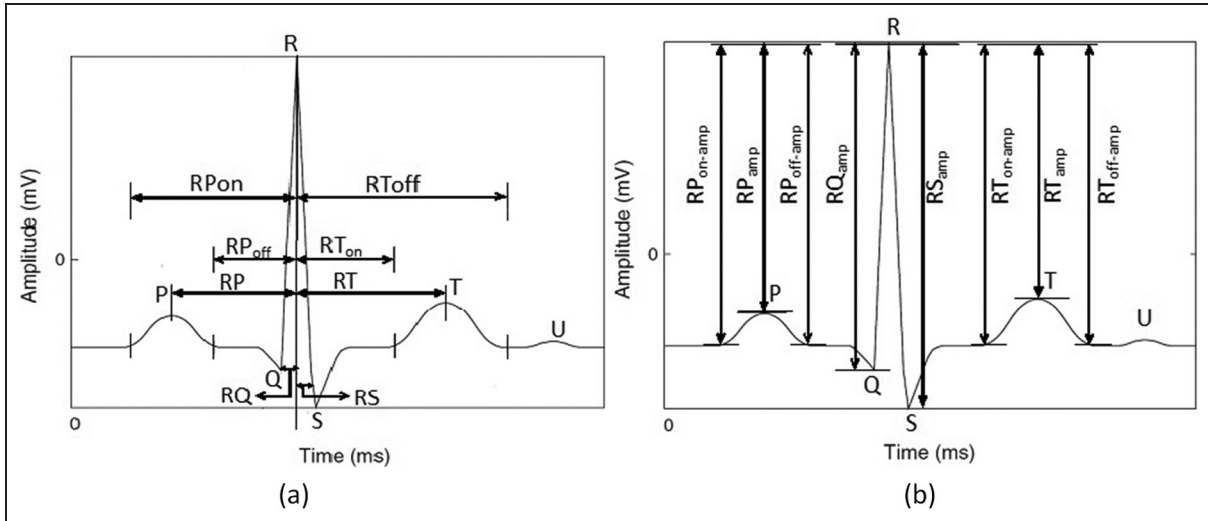


Figure 5. Extracted interval (a) and amplitude (b) features from ECG fiducial points.

obtained results consisted of Q, R, and S peaks along with their corresponding time indexes. Consequently, the beat interval was measured from each R peak to the next (RR).

A wave segmentation method³⁰ was then used to find P and T wave peaks by searching for local maxima within a pre-defined distance from QRS peaks. The search intervals for P and T were heuristically identified. The P wave peak is assumed to be located within a third of RR interval to the next QRS onset, while the T wave peak is located within half the RR interval from QRS offset. Additional points representing onset and offset of T and P waves were also detected using the minimum radius of curvature, which is more robust to noise and artifacts than derivative search methods. Figure 5 illustrates the different identified fiducial points (P, P_{on}, P_{off}, Q, R, S, T, T_{on}, and T_{off}) along with possible extracted features in reference to the prominent peak R.

4.4. Feature selection

From the detected fiducial points, various amplitude and interval features can be extracted; however, the curse of dimensionality can inherently affect classification and redundant attributes may lead to higher computational cost and complexity. Therefore, feature selection seeks to reduce the number of attributes by selecting minimal efficient feature subsets from the identified fiducial points.

We utilized filter-based methods to select features namely Fischer score and information gain, which are independent assessment approaches based on characteristic data. The methods rank each feature according to some metric and select the features with highest scores; these scores show the discriminative power of each attribute. The Fisher score selects features that assign similar values to the samples from the same class and different values to

samples from different classes. The Fischer score method ranks features based on the following score function:

$$F_r = \frac{\sum_{i=1}^c l_i (\mu_r^i - \mu_r)^2}{\sum_{i=1}^c l_i (\sigma_r^i)^2} \quad (1)$$

where l_i denote the number of samples in class i , and μ_r^i and σ_r^i are the mean and standard deviation of class i , ($i = 1, \dots, c$) corresponding to the r th feature.

Information gain evaluates features by measuring their information gain with respect to the class, which is calculated by entropy. The joint entropy about attribute X and class Y is calculated as follows:

$$I(i) = \sum_{x_i} \sum_y P(X=x_i, Y=y) \log \frac{P(X=x_i, Y=y)}{P(X=x_i)P(Y=y)} \quad (2)$$

Using these two methods, we eliminated common extraneous features with the lowest scores. However, it was also important to check for correlation between features to prevent feature redundancy and to lower computational cost. We used Pearson correlation coefficient (PCC) to measure the linear dependency between features, which is calculated as follows:

$$\text{correl}(X, Y) = \frac{\sum (x - \bar{x})(y - \bar{y})}{\sqrt{\sum (x - \bar{x})^2 \sum (y - \bar{y})^2}} \quad (3)$$

For each of the ECG signal intervals, PR interval, QRS interval and RT interval, highly correlated features were reduced to only one. For instance, the correlated intervals RP_{onset}, RP, and RP_{offset} were substituted by RP; and the correlated amplitudes RP_{onset-amp}, RP_{amp}, and RP_{offset-amp} by RP_{amp}. The resulting subset contained eight features

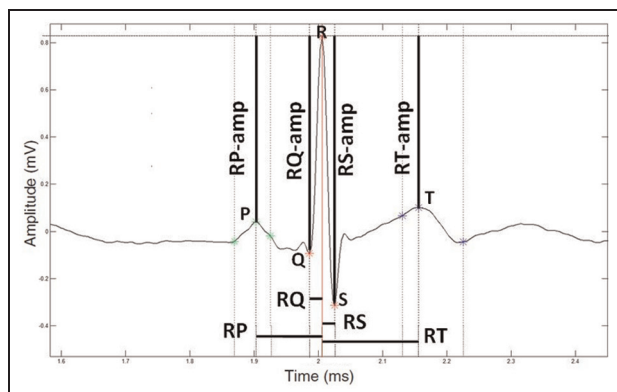


Figure 6. Selected amplitude and interval features.

highly correlated with the class, yet uncorrelated with each other; the selected features are shown in Figure 6.

4.4. Classification

Classification aims to map instances of the 8th dimensional selected feature vector to the appropriate auscultation classes. Numerous machine learning methods have been employed for supporting decision making in medical research and diagnosis based on probabilistic or statistical models.³¹

The first classifier is naive Bayes, which assumes a strong conditional independence among the features. Second is Bayes' network classifier with augmented edges to the simple naive Bayes classifier; this classifier was constructed by the Tree Augmented Naïve Bayes (TAN) algorithm. Another classifier used is k -nearest neighbor (KNN), which is instance-based. It uses the Euclidean distance to find closest training instances to the test sample and predicts the class. A C4.5 decision tree classifier, which is one of the most widely used and practical methods for inductive inference, was also tested. This decision tree classifier is for approximating discrete-valued functions; it is known to be robust to noisy data and capable of learning disjunctive expressions. Lastly, we used multiple layer perceptron (MLP), which is an artificial neural network (ANN) based classifier consisting of a simple neuron-like processing unit interconnected to simulate human neurons. All classifiers were implemented in a freely available software package WEKA,³² an open-source data mining application with large collection of classification, clustering and feature processing algorithms.

5. Results and discussion

Each single ECG run had a duration of 10 seconds resulting in approximately 10 heart pulses per signal; however, to preserve complete heart beat signals, the first and last

Table 1. Auscultation areas classification of all various angles using naive Bayes.

Lead angle (degrees)	Orientation Diagram	Classifier accuracy (%) (three-fold cross-validation)	
		Standardized Patient 1	Standardized Patient 2
0°		100	100
45°		100	100
90°		100	100
135°		97	99
180°		98.8	98.2
225°		100	96.5
270°		99.4	100
315°		99	99.4

pulses were removed, as detailed in Section 4.1. After recording 5 runs at each orientation, each auscultation area consisted of about 320 pulses. Thus, ECG analysis of each SP comprised a total of 1280 pulses.

The preprocessing of ECG signals, which consisted of denoising and filtering, successfully preserved the ECG signal boundaries, even in the existence of strong power-line and baseline wandering noises, as previously illustrated in Figure 4. ECG fiducial points were identified after using the Pan–Tompkins algorithm for QRS complex detection and wave segmentation for P and T wave delineation. The numerous features extracted from the fiducial points were then reduced using feature selection methods, keeping only relevant and non-redundant information.

In our previous work,² we were able to accurately classify the four auscultation areas with the stethoscope diaphragm fixed at the same orientation. The orientation comprised of the two electrodes positioned horizontally, considered as 0° angle. Here, we first extended the previous work to classify the four auscultation areas with the stethoscope diaphragm positioned at several orientations with 45° increments. Based on the selected eight features of each pulse, a three-fold cross-validation of the naive Bayes classifier was conducted. Highly accurate results were obtained as shown in table 1; hence, it was not required to utilize any other classifier at this step.

To account for trainee's distinctive stethoscope head placement and assess orientation-invariability, we combined all instances collected at different diaphragm positions. For data visualization, the selected features were reduced to two using principle component analysis (PCA) and all instances of the four auscultation areas for both SPs were plotted as illustrated in Figure 7.

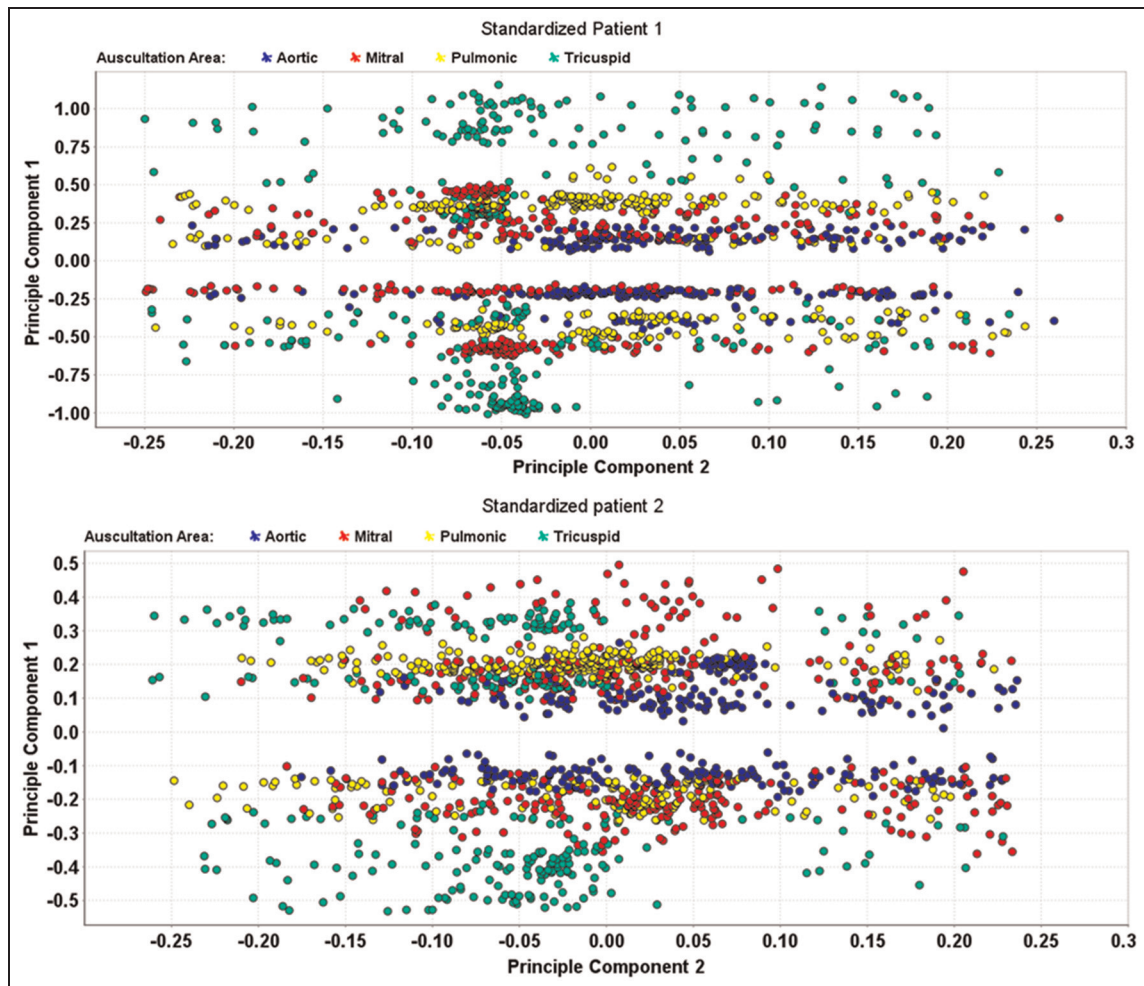


Figure 7. Data visualization of all ECG pulses using PCA for SP1 and SP2.

Table 2. Auscultation areas classification for any stethoscope diaphragm orientation.

SP	Classifier accuracy (%) (10-fold cross-validation)				
	Naive Bayes	Bayes network	k-nearest neighbor (5-NN)	Decision tree (C4.5)	Multilayer perceptron (MLP)
1	60.40	92.20	89.03	95.14	84.17
2	60.03	86.89	79.94	87.11	79.94

For classification, we applied a 10-fold cross-validation on several classifiers, naive Bayes, Bayes network, KNN, MLP and C4.5 decision tree; the obtained results are illustrated in Table 2. The C4.5 decision tree performed the best with an accuracy of 95.1% and 87.1% for SP1 and SP2, respectively; this method was a one-step look ahead and non-backtracking search through the space of all possible decision trees. The Bayes network with TAN also produced adequate results with an accuracy of 92.2% and 86.9% for SP1 and SP2, respectively. Confusion matrices

of our best classifier, C4.5 decision tree, for both SPs are shown in Tables 3 and 4.

6. Conclusion

In this work, we have investigated the application of an orientation invariant ECG-based virtual pathology stethoscope tracking method for placing virtual symptoms in correct auscultation landmarks of SPs. Two electrodes attached on the stethoscope diaphragm were used to collect ECG

Table 3. C4.5 decision trees classifier confusion matrix for SP1.

Predicted areas	Known auscultation areas			
	Aortic	Mitral	Pulmonic	Tricuspid
Aortic	327	5	4	2
Mitral	7	310	9	12
Pulmonic	5	6	334	3
Tricuspid	2	7	4	321

Table 4. C4.5 decision trees classifier confusion matrix for SP2.

Predicted areas	Known auscultation areas			
	Aortic	Mitral	Pulmonic	Tricuspid
Aortic	312	20	12	3
Mitral	23	324	18	27
Pulmonic	15	20	309	9
Tricuspid	4	21	10	284

from four auscultation regions, aortic, mitral, pulmonic, and tricuspid, of two male SPs. Since trainees may place the stethoscope head at different angles when performing auscultation, ECG signals were collected rotating the stethoscope diaphragm clockwise with 45° increments, producing eight different orientations for each auscultation area.

ECG signals were first preprocessed to remove noise and other artifacts. Numerous features were then extracted and relevant features were selected for classification. Several classifiers, using various algorithmic approaches, were utilized to assess the discriminative abilities and orientation-invariability of the system. Imposing results of 95.1% accuracy for SP1 and 87.1% for SP2 were obtained establishing accurate classification of the four different auscultation areas. These results are impressive since they do not yet consider the prior information of trainees holding the stethoscope in a particular auscultation area for several seconds before moving to another; this knowledge can be useful to calculate the *a posteriori* probabilities. The promising findings would significantly aid in extending the capabilities of SPs and allow medical student trainees to perform realistic auscultation and hear abnormal heart or lung sounds in otherwise healthy patient actors.

For future work, we will consider real-time applications utilizing sequential beat classification leveraging intermittent movement of the stethoscope. Also, a larger pilot study with diverse SPs, including female test subjects, is to be conducted to investigate population invariability. The work can be further extended to cover additional cardiac and pulmonary auscultation regions.

References

1. Vukanovic-Criley JM, Criley S, Warde CM, et al. Competency in cardiac examination skills in medical students,

trainees, physicians, and faculty: a multicenter study. *Arch Intern Med* 2006; 166(6): 610.

2. Weaver M and Erby L. Standardized patients A promising tool for health education and health promotion. *Health Promotion Practice* 2012; 13(2): 169-174.
3. Bramstedt KA, Moolla A and Rehfield PL. Use of standardized patients to teach medical students about living organ donation. *Prog Transplant* 2012; 22(1): 86-90.
4. Marken PA, Zimmerman C, Kennedy C, Schremmer R and Smith KV. Human simulators and standardized patients to teach difficult conversations to interprofessional health care teams. *Am J Pharmaceut Educ* 2010; 74(7): 120.
5. May W, Park JH and Lee JP. A ten-year review of the literature on the use of standardized patients in teaching and learning: 1996-2005. *Med Teacher* 2009; 31(6): 487-492.
6. Kidane N, Chemlal S, Hubbard T and McKenzie FD. Using EKG signals for virtual pathology stethoscope tracking in standardized patient heart auscultation. In *2011 IEEE 37th Annual Northeast Bioengineering Conference (NEBEC)*. IEEE, 2011, pp. 1-2.
7. Clifford GD, Azuaje F and McSharry P. *Advanced methods and tools for ECG data analysis*. London: Artech House, 2006.
8. Agrafioti F, Hatzinakos D and Anderson AK. ECG pattern analysis for emotion detection. *IEEE Trans Affective Comput* 2012; 3(1): 102-115.
9. Wu W and Lee J. Improvement of HRV methodology for positive/negative emotion assessment. In *5th International Conference on Collaborative Computing: Networking, Applications and Worksharing, 2009 (CollaborateCom 2009)*. IEEE, 2009, pp. 1-6.
10. De Chazal P, Heneghan C, Sheridan E, Reilly R, Nolan P and O'Malley M. Automated processing of the single-lead electrocardiogram for the detection of obstructive sleep apnoea. *IEEE Trans Biomed Eng* 2003; 50(6): 686-696.
11. McKenzie FD, Garcia HM, Castelino RJ, Hubbard TW, Ullian JA and Gliva GA. Augmented standardized patients now virtually a reality. In *Third IEEE and ACM International Symposium on Mixed and Augmented Reality, 2004. ISMAR 2004*. IEEE, 2004, pp. 270-271.
12. Karnath B and Thornton W. Auscultation of the Heart. *Hospital Physician* 2002; 38(9): 39-45.
13. Malmivuo J and Plonsey R. *Bioelectromagnetism: principles and applications of bioelectric and biomagnetic fields*. New York: Oxford University Press, 1995.
14. Richardson TR and Moody JM Jr. Bedside cardiac examination: constancy in a sea of change. *Curr Problems Cardiol* 2000; 25(11): 783.
15. Chizner MA. Cardiac auscultation: rediscovering the lost art. *Curr Problems Cardiol* 2008; 33(7): 326.
16. Finley JP, Sharratt GP, Nanton MA, Chen RP, Roy DL and Paterson G. Auscultation of the heart: a trial of classroom teaching versus computer-based independent learning. *Med Educ Oxford* 1998; 32: 357-361.
17. Vukanovic-Criley JM, Boker JR, Criley SR, Rajagopalan S and Criley JM. Using virtual patients to improve cardiac examination competency in medical students. *Clin Cardiol* 2008; 31(7): 334-339.
18. Criley JM, Keiner J, Boker JR, Criley SR and Warde CM. Innovative web-based multimedia curriculum improves

- cardiac examination competency of residents. *J Hospital Med* 2008; 3(2): 124–133.
19. Ward JJ and Wattier BA. Technology for enhancing chest auscultation in clinical simulation. *Resp Care* 2011; 56(6): 834–845.
 20. Maran NJ and Glavin RJ. Low-to high-fidelity simulation—a continuum of medical education? *Med Educ* 2003; 37(S1): 22–28.
 21. Issenberg SB, Gordon MS and Greber AA. Bedside cardiology skills training for the osteopathic internist using simulation technology. *JAOA* 2003; 103(12): 603–607.
 22. Guirlinger SR. *Simulation to Augment Standardized Patients in Obstetric Ultrasound Training*. PhD dissertation, Old Dominion University, 2007.
 23. Kneebone R, Kidd J, Nestel D, Asvall S, Paraskeva P and Darzi A. An innovative model for teaching and learning clinical procedures. *Med Educ* 2002; 36(7): 628–634.
 24. Israel SA, Irvine JM, Cheng A, Wiederhold MD and Wiederhold BK. ECG to identify individuals. *Pattern Recognition* 2005; 38(1): 133–142.
 25. Islam MS, Alajlan N, Bazi Y and Hichri HS. HBS: a novel biometric feature based on heartbeat morphology. *IEEE Trans Informat Technol Biomed* 2012; 16(3): 445–453.
 26. Singh YN and Gupta P. Correlation-based classification of heartbeats for individual identification. *Soft Comput* 2011; 15(3): 449–460.
 27. Luo S and Johnston P. A review of electrocardiogram filtering. *J Electrocardiol* 2010; 43(6): 486.
 28. Kohler B-U, Hennig C and Orglmeister R. The principles of software QRS detection. *IEEE Engng Med Biol Mag* 2002; 21(1): 42–57.
 29. Pan J and Tompkins WJ. A real-time QRS detection algorithm. *IEEE Trans Biomed Engng* 1985; 3: 230–236.
 30. Espiritu-Santo-Rincon A and Carbajal-Fernandez C. ECG feature extraction via waveform segmentation. In *2010 7th International Conference on Electrical Engineering Computing Science and Automatic Control (CCE)*. IEEE, 2010, pp. 250–255.
 31. Witten IH and Frank E. *Data Mining: Practical machine learning tools and techniques*. San Mateo, CA: Morgan Kaufmann, 2005.
 32. Hall M, Frank E, Holmes G, Pfahringer B, Reutemann P and Witten IH. The WEKA data mining software: an update. *ACM SIGKDD Explorations Newsletter* 2009; 11(1): 10–18.

Author biographies

Nahom Kidane is a PhD candidate in the Modeling, Simulation and Visualization Engineering (MSVE) Department at Old Dominion University. He received a bachelor degree in Electrical Engineering from Jimma University, Jimma, Ethiopia and MS in Modeling and Simulation from Old Dominion University. His research interests include virtual reality applications for medical and human training, modeling and simulation, machine learning and medical image processing.

Salim Chemlal is a PhD candidate in the Electrical and Computer Engineering Department at Old Dominion University.

He received dual bachelor degrees in Electrical and Computer Engineering and MS in Modeling and Simulation from Old Dominion University. His areas of interest include medical modeling and simulation, mhealth applications, machine learning and manifold learning algorithms, and augmented reality and scientific visualization. To date, his projects in these areas have led to several publications and outstanding awards.

Jiang Li received his PhD degree in Electrical Engineering from the University of Texas at Arlington, TX, in 2004, the MS degree in Automation from Tsinghua University, China, in 2000, and the BS degree in Electrical Engineering from Shanghai Jiaotong University, China, in 1992. His research interests include machine learning, computer-aided medical diagnosis systems, medical signal/image processing, neural network and modeling and simulation. He has published more than 50 journal and conference papers. He is a reviewer for several journals and a guest associate editor for *Medical Physics*. He worked as a post-doctoral fellow at the department of radiology, National Institutes of Health, from 2004 to 2006. He joined ODU as an assistant professor in Spring 2007. He is also affiliated with Virginia Modeling, Analysis, and Simulation Center (VMASC). He is a member of the IEEE and the Sigma Xi.

Rick McKenzie is a Professor and Chair of the Modeling, Simulation and Visualization Engineering (MSVE) Department and a joint faculty member in the Department of Electrical and Computer Engineering (ECE) at Old Dominion University in Norfolk, Virginia U.S.A. In addition, he is co-director of the Medical Imaging, Diagnosis, and Analysis (MIDA) Laboratory at ODU and Adjunct Associate Professor of Eastern Virginia Medical School (EVMS) in the School of Health Professions. Before coming to Old Dominion University, he spent 6 years in the simulation industry at Science Applications International Corporation (SAIC) as a senior scientist. He has a BS in Engineering, MS in Computer Engineering and a PhD in Computer Engineering, all from the University of Central Florida in Orlando, Florida. His research has been in medical modeling and simulation, human behavior representation, and simulation architectures often focusing on aspects of scientific visualization and virtual reality.

Thomas W. Hubbard is Professor of Clinical Pediatrics at Eastern Virginia Medical School and Director of Sentara Center for Simulation and Immersive Learning. He has a BA in Psychology with a minor in Biology from the University of Virginia, MD from Eastern Virginia Medical School, MPH from the University of Pittsburgh and JD from the Marshall Wythe School of Law of the College of William and Mary. His research interests include clinical studies of tinea capitis, vaccine trials and applying simulation technologies in medical education. He has published widely in medical journals including *The New England Journal of Medicine*, *Pediatrics*, *American Journal of Diseases in Children*, and *Trauma*. He has served on the editorial board of *Trauma* and is currently a reviewer for *Pediatrics and Academic Medicine*.